



**Research Paper / Makale**

**Recognition of Tire Track Patterns Using SIFT and Template Matching**

Asuman GÜNAY YILMAZ<sup>1a</sup>, Ekrem İBRAM<sup>1</sup>, Vasif NABİYEYEV<sup>2b</sup>

<sup>1</sup>Department of Software Engineering, Karadeniz Technical University, Trabzon, Turkey

<sup>2</sup>Department of Computer Engineering, Karadeniz Technical University, Trabzon, Turkey  
[gunaya@ktu.edu.tr](mailto:gunaya@ktu.edu.tr)

**Received/Geliş:** 02.09.2021

**Accepted/Kabul:** 05.11.2021

**Abstract:** Recognition of tire track patterns has an important role in both the investigation of crime scenes and the identification of vehicles involved in traffic accidents. Due to the rich texture information they have, texture features are generally used to recognize track images taken from tires. However, recognition of tire tracks taken from crime scenes has not been studied sufficiently. In this study, SIFT-based features and template matching methods were used to recognize tire track/tire track fragment images. In the experiments, fragments taken from clean tracks, dirty tracks and fragments taken from dirty tracks were matched with clean track images, and higher recognition performance was achieved compared to state of art methods.

**Keywords:** Tire track image, SIFT, template matching

**SIFT ve Şablon Eşleme ile Lastik İzi Desenlerinin Tanınması**

**Öz:** Lastik izi desenlerinin tanınması hem suç olay mahallerinin araştırılmasında hem de trafik kazalarında kazaya karışan araçların belirlenmesinde önemli role sahiptir. Taşıdığı zengin doku bilgisi nedeniyle lastiklerden alınan desen görüntülerinin tanınmasında doku öznelikleri kullanılmaktadır. Fakat olay yerlerinden alınan lastik izlerinin tanınması konusu yeterince çalışılmamıştır. Bu çalışmada lastik izi/iz parçası görüntülerinin tanınması amacıyla SIFT tabanlı öznelimler ve şablon eşleme yöntemleri kullanılmıştır. Deneylerde temiz izlerden alınan kesitlerin kirlizden ve kirlizden alınan kesitlerin, temiz izlerle eşleştirilmesi işleminde literatürdeki yöntemlere göre daha yüksek tanıma başarımları elde edilmiştir.

**Anahtar Kelimeler:** Lastik izi görüntüsü, SIFT, şablon eşleme

**1. Introduction**

The use of vehicles during criminal activities often leaves tire tracks at crime scenes. Therefore, tire tracks can be used to detect vehicles involved in these crimes. In addition, tire tracks can provide important evidence in determining the responsibilities of drivers in traffic accidents. Manually detecting vehicles from tire tracks is hard and may have a low success rate. For this reason, various scientific studies are carried out on tire tracks/pattern recognition.

Tire pattern images are usually dark gray, the edges of the pattern are clearly defined, and these images have rich texture information. Therefore, feature extraction methods can be used successfully in the representation of tire patterns. Rotation, lighting, and scale-independent feature extraction methods are generally used in this area. Tire track images taken from crime scenes, on the other hand, vary considerably depending on the structure of the ground (soil, asphalt, sand, snow, rain, mud, etc.). In the literature it can be seen that the studies are limited and mostly focused

*How to cite this article*

Günay Yılmaz, A., İbrahim, E., Nabiyev, V., "Recognition of Tire Track Patterns Using SIFT and Template Matching" El-Cezeri Journal of Science and Engineering, 2022, 9 (2); 634-643.

*Bu makaleye atıf yapmak için*

Günay Yılmaz, A., İbrahim, E., Nabiyev, V. "SIFT ve Şablon Eşleme ile Lastik İzi Desenlerinin Tanınması" El-Cezeri Fen ve Mühendislik Dergisi 2022, 9 (2); 634-643.

ORCID ID: <sup>a</sup>0000-0003-3960-5085; <sup>b</sup>0000-0003-0314-8134

on the pattern images taken from tires. But the studies using directly the tire track images are very few. The reason for the limited number of studies on the classification of tire patterns is the lack of standard data sets and the difficulty of data collection. Researchers often have to conduct experiments on datasets that they collect, which contain small number of images.

Colbry et al. [1] extracted features from tire pattern images with 2D-FFT (Fast Fourier Transform), reduced the feature size with PCA (Principal Component Analysis) and classified them with KNN (k-nearest neighbor) classifier to automate the tire pattern recognition process. The aim of the study is to extract images from the dataset similar to the test image. For the data set consisting of 90 tire pattern images, the number of images to be compared with the test image has been reduced to 60. In Huang et al. study [2], straight (frontal and upright) tracks were obtained by manually rotating the tire track images. The gaps in track images were filled with morphological opening process. Then, the number of grooves of tires was determined using the horizontal projection of tracks. 2-groove, 3-groove and 4-groove tires were classified with separate SVM (Support Vector Machine) classifiers. The wavy tracks were classified by extracting Gabor features in various directions and scales and using a separate SVM classifier. Their dataset was consisting of 15 tire track images. These images were mirrored horizontally and vertically to increase the number of data. They achieved 60% classification accuracy for tire track images. Bulan et al. [3], classified tire images as winter, summer and all-season. After determining the tire part from the images, the edges were extracted with Canny edge detection method and then FFT was applied. After feature extraction using PCA, they were classified using SVM. The database consists of images with different lighting conditions and different shooting angles (140 winter, 70 all-season, 70 summer tire images). The tests were carried out on two classes, and 97.86% success was achieved in the determination of winter tires, 84.79% in the determination of all-season tires and 93.36% in the determination of summer tires.

Wang et al. [4] applied a two-level wavelet transform to the tire pattern images for the purpose of tire pattern retrieval. The low frequency sub bands were eliminated, and the features were extracted by SIFT (Scale Invariant Feature Transform) by reconstructing the images from 6 high frequency sub bands. In the experiments improvement in retrieval time was achieved on the database consisting of 200 tire pattern images in 40 categories. Liu et al. [5] extracted rotation invariant features from the tire image database using Radon transform and Curvelet transform for image retrieval purposes. Experiments were carried on the dataset containing 200 tire pattern images in 40 categories, and the retrieval speed was improved. Ge et al. [6] extracted features with the HoG (Histogram of Gaussian) domain texture tendency method for tire pattern retrieval. The database consists of 1035 tire pattern images obtained from different environments. Experiments were carried out on different number of datasets (100, 500, 1000, 5000, 10000) using images containing different lighting conditions, scale, rotation angle and their combinations. In the study, 81.21% retrieval success was achieved.

Liu et al. [7] published the first study that used CNN (Convolutional Neural Network) for feature extraction in tire pattern classification. The features from the last two layers of CNN were combined with different weights and the size of the feature space was reduced using PCA. Then these features were used to train a SVM classifier. They achieved 79.6% success rate on a database containing 100 classes and 5000 images. Liu et al. [8] produced sub bands using DWT (Discrete Wavelet Transform) from tire pattern images and reproduced images with inverse transform (IDWT) in each sub band. The features were extracted from these 4 sub-band images using LBP (Local Binary Patterns) and combined with different weights. While extracting the features with LBP, 16 neighbors at 2 pixels distance from the center pixel (5x5 region) were evaluated, and thresholding was made according to the average value of the 5x5 region instead of the center pixel. In the study, the rotation invariant features were used, and 82.6% success was achieved in the tire pattern dataset consisting of 5000 images of 100 classes. Wang et al. [9], on the other hand, used the GCN (Gabor

Convolutional Network) by adding Gabor filters to the deep learning model for tire pattern classification. Experiments were conducted with multi-scale Gabor CNN on the database consisting of 100 classes and 5000 images, and 95.9% success rate was achieved.

As stated before, the recognition of full or partial tire tracks left by the vehicles at the crime scenes provides important information in determining the characteristics of the vehicles. However, a few studies were made on tire track recognition in the literature. In addition, most of the studies are trying to classify tire patterns through images taken directly from tires. The number of studies on the recognition of tire tracks is negligible. In this study, it is aimed to classify the full tire track/tire track fragment images. For this purpose, full tire track images were collected from the internet, fragments of various sizes were taken from these tracks and tried to match them with full tracks. In addition, dirty tracks were produced from the tire track images and the dirty tracks were matched with the clean tracks. Finally, the fragments taken from the dirty tracks were recognized. The flow diagram of the tire track recognition process used in the study is given in Figure 1. As seen in the figure, keypoints were determined using SIFT from the tire track images and clean/dirty tire track fragment images. Then, the outliers were eliminated using the RANSAC (Random Sample Consensus) algorithm to increase the accuracy of the matches. On the other hand, the template matching method was also used to find the similarity of the tracks.

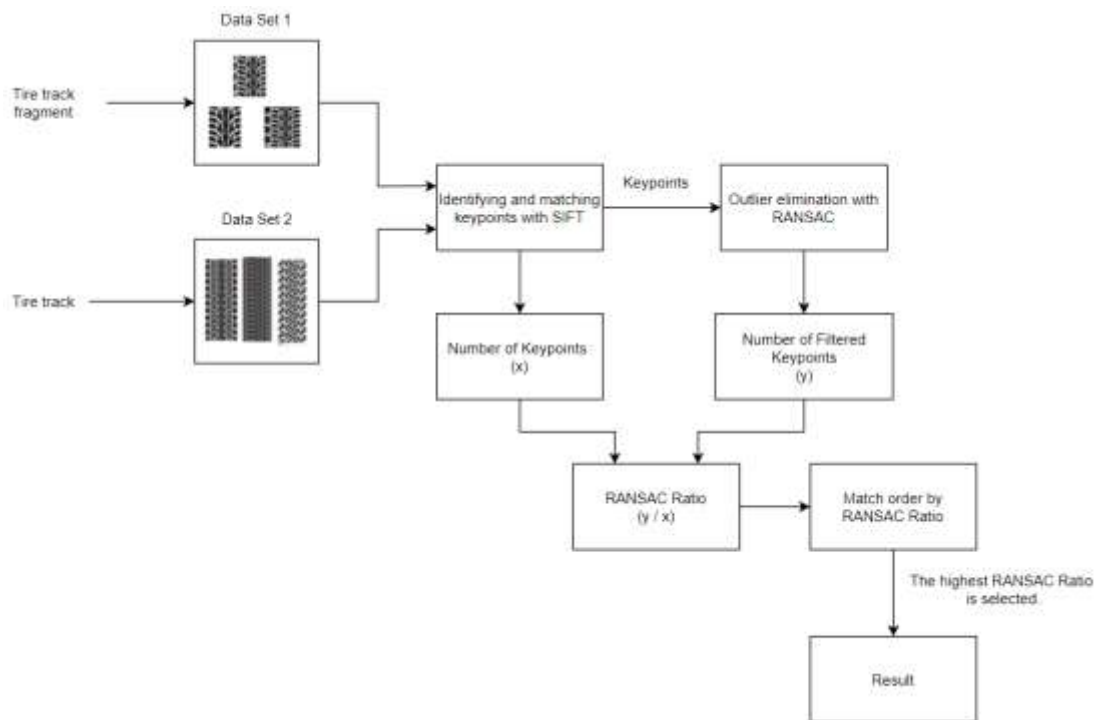


**Figure 1.** The flow diagram of the tire track recognition system

The rest of the paper is organized as follows. In Section 2, the dataset and the method are explained. The experimental results are given in Section 3, and the conclusions are outlined in Section 4.

## 2. Material and Method

### 2.1. Dataset

The dataset was collected from the sites that provide tire track images over the internet [10]. Our dataset consists of 4 groups: clean tracks, clean track fragments, dirty tracks and dirty track fragments. The group consisting of 35 tire track images is called clean tracks. Three fragments in different sizes were taken from each clean track, and a 105-element image set, named clean track

fragments, was obtained. Then, 35 dirty tracks were obtained by randomly using black or white colored spray brushes on clean tracks. Here, it is ensured that data loss with white spraying and adding data with black spraying is provided to black density track images. On the other hand, the process is opposite for white density track images. Finally, 3 different sized fragments were taken from the dirty track images and 105 dirty track fragments were obtained. Sample images from the dataset are given in Figure 2. The SIFT-RANSAC and template matching methods are explained in the next subsections.

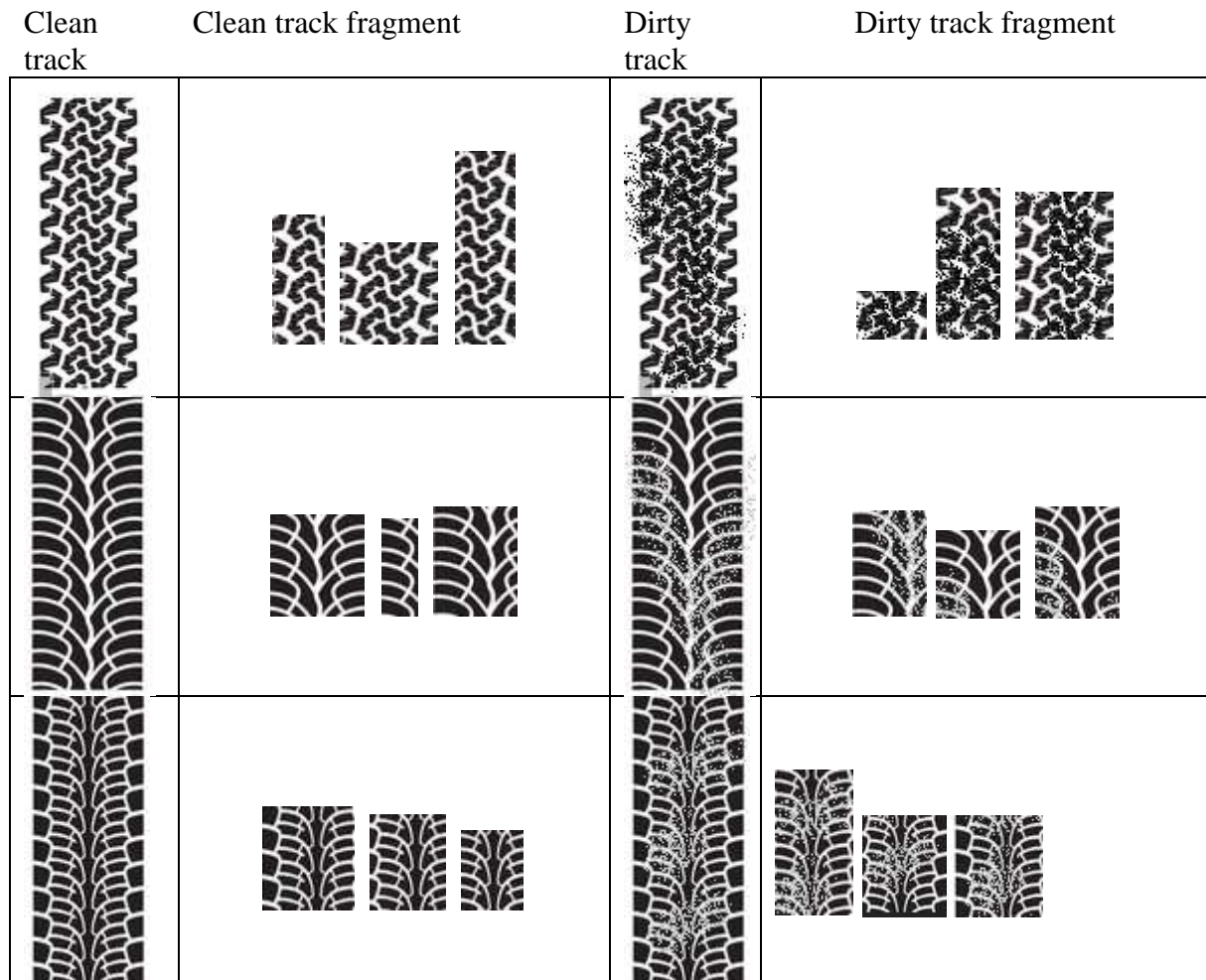


**Figure 2.** Sample images from the dataset

## 2.2. Feature Extraction with SIFT

Scale Invariant Feature Transform (SIFT) which is developed by David Lowe [11, 12] is an image descriptor for image-based matching and recognition applications. SIFT features are not affected by transformations in the image such as translation, rotation, and scaling. Experimentally, the SIFT descriptor has proven to be very effective in real world applications such as image matching and object recognition.

### 2.2.1. Scale-space Extrema Detection

SIFT algorithm is based on detecting the positions in the image which are called keypoints. The image is processed with Gaussian filters at different scales and then the difference of consecutive filtered images is taken (DoG-Difference of Gaussian). The maximum/minimum points (scale space extrema) in these difference images are determined as keypoints. Keypoint detection is performed by comparing each pixel in the DoG images with its eight neighbors at the same scale and its

corresponding nine neighbors at each of the neighboring scales. If the pixel value is the maximum or minimum among all compared pixels, it is selected as a keypoint candidate. Specifically, a DoG image  $D(x, y, \sigma)$  is obtained by Equation 1.

$$D(x, y, \sigma) = L(x, y, k_i\sigma) - L(x, y, k_j\sigma) \quad (1)$$

Here  $L(x, y, k\sigma)$  is the filtering of the original image  $I(x, y)$  on the  $k\sigma$  scale with the Gaussian filter (Equation 2).

$$L(x, y, k\sigma) = G(x, y, k\sigma) * I(x, y) \quad (2)$$

### 2.2.2. Keypoint Localization

Scale space extrema detection results in the generation of a large number of keypoint candidates, some of which are unstable. The next step in the algorithm is to perform a detailed fit to the nearby data for accurate position, scale, and principal curvature. This information allows points of low contrast (and therefore sensitive to noise) or poorly localized along an edge to be rejected.

### 2.2.3. Orientation Assignment

In this step, each keypoint is assigned one or more orientations based on local image gradient directions. This is the key step in achieving the rotation invariance property, as the keypoint identifier can be represented according to these orientations and thus ensures invariance in the image rotation transformation. Gaussian-smooth filtered image  $L = (x, y, \sigma)$  of the keypoint in  $\sigma$  scale is taken. For an image sample in  $\sigma$  scale  $L = (x, y)$ , the pixel differences of gradient magnitude  $m = (x, y)$  and orientation  $\theta = (x, y)$  are calculated using the following equations.

$$m(x, y) = \sqrt{(L(x+1, y) - L(x-1, y))^2 + (L(x, y+1) - L(x, y-1))^2} \quad (3)$$

$$\theta = (x, y) = \text{atan2}(L(x, y+1) - L(x, y-1), L(x+1, y) - L(x-1, y)) \quad (4)$$

Magnitude and orientation calculations are made for each pixel in the neighboring region around the keypoint in the Gaussian-blur filtered image.

### 2.2.4. Keypoint Descriptor

After determining the keypoint locations and orientations at certain scales, an identifier vector is calculated for each keypoint. First, a series of orientation histograms are generated in 4x4 pixel neighborhood. Each histogram is calculated from the magnitude and orientation values of the samples in the 16 x 16 region around the keypoint, including samples from the 4x4 subregion of the original neighboring region.

In the study the similarity of tire track images was calculated based on the matching of keypoint identifiers. Then the RANSAC method was used for the elimination of outliers in these matches.

## 2.3. Outlier Elimination with RANSAC

Random sample consensus (RANSAC) [13] is an iterative method for estimating the parameters of a mathematical model from a set of observed data containing outliers where outliers have no effect

on the predicted values. Therefore, it can also be interpreted as an outlier detection method. The RANSAC algorithm basically consists of two iterative steps.

In the first step, a sample subset containing the minimum data items is randomly selected from the input dataset. A suitable model and corresponding model parameters are calculated using only the elements of this subset of samples. In the second step, the algorithm checks which elements of the entire dataset are consistent with the model produced with the estimated model parameters obtained from the first step. A data item is considered an outlier if it does not fit this model according to a given error threshold (Figure 3). The set of inliers obtained for the fitting model is called the consensus set. The RANSAC algorithm iteratively repeats these two steps until the consensus set obtained in a given iteration has enough inliers.

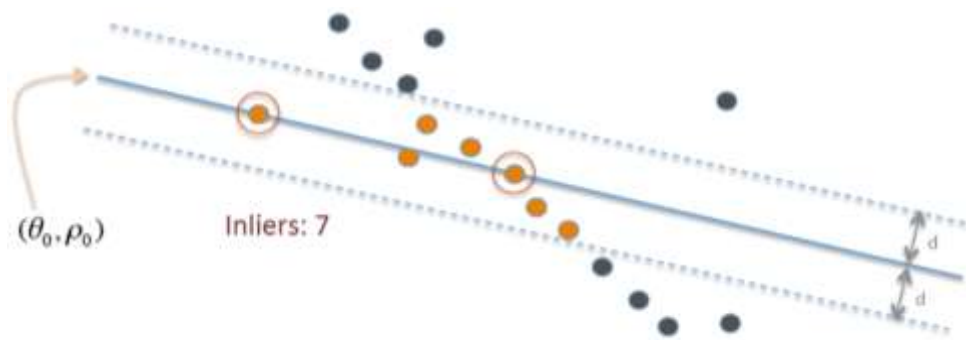


**Figure 3.** The threshold value produced with RANSAC algorithm to detect outliers [14]

In this study, we try to recognize tire tracks by using different data groups in the experiments. In the method, firstly, keypoints are obtained from the input tire track image and all track images in the dataset using SIFT and matched. The number of matches obtained ( $x_i$ ) is kept. Then, the RANSAC algorithm is applied to eliminate the outliers in keypoint matches. The number of keypoint matches remaining after this elimination ( $y_i$ ) is also kept. Finally, the  $r_i = y_i/x_i$  ratio is calculated and transferred to the match list created for that track. As a result of the comparisons, the image with the highest ratio in the list is determined as the track that matches the input image.

## 2.4. Template Matching

Template matching is a method for finding the input part in a larger image [15]. The piece of an image given as input is shifted pixel by pixel on the large image to check whether the images are matched. According to the match rate returned from the compared pixels, it is determined where the part was taken from.

In the study, the input image is shifted pixel by pixel on each image in the dataset. For each step, the proportion of pixels matching the input image is calculated. The highest match rate obtained is added to the list. When the process is completed for all images in the dataset, the track with the highest value among the ratios in the list is selected as the track that matches the input image.

## 3. Experiments and Results

In this section, the experiments performed on the dataset and the results are explained. Our dataset consists of 280 images, including 35 clean tracks, 35 dirty tracks, 105 clean track fragments and 105 dirty track fragments. Various test scenarios have been created for these images. The test scenarios used in the experiments are given in Table 1. In scenario A, clean track fragments were

matched with clean tracks. The scenarios of matching dirty track fragments with clean tracks and dirty tracks with clean tracks are named as scenario B and C, respectively. Performance rates for each test scenario were calculated using SIFT and template matching methods.

**Table 1.** Test scenarios

Test Scenario	Data group 1	Data group 2
A	Clean track fragments	Clean tracks
B	Dirty track fragments	Clean tracks
C	Clean tracks	Clean tracks

An example image showing the keypoints of two clean track fragments matching the clean track according to test scenario A is given in Figure 4a. The figure shows the keypoints (produced and matched by SIFT) of two different sized fragments taken from the same track. After eliminating the outliers in these keypoint matches, the position of the fragment on the track image is determined more clearly according to the remaining key point matches as seen in Figure 4b.

The sample track images for the keypoint matches obtained by SIFT for test scenarios B and C and the keypoint matches after outlier elimination are shown in Figure 5 and Figure 6, respectively.

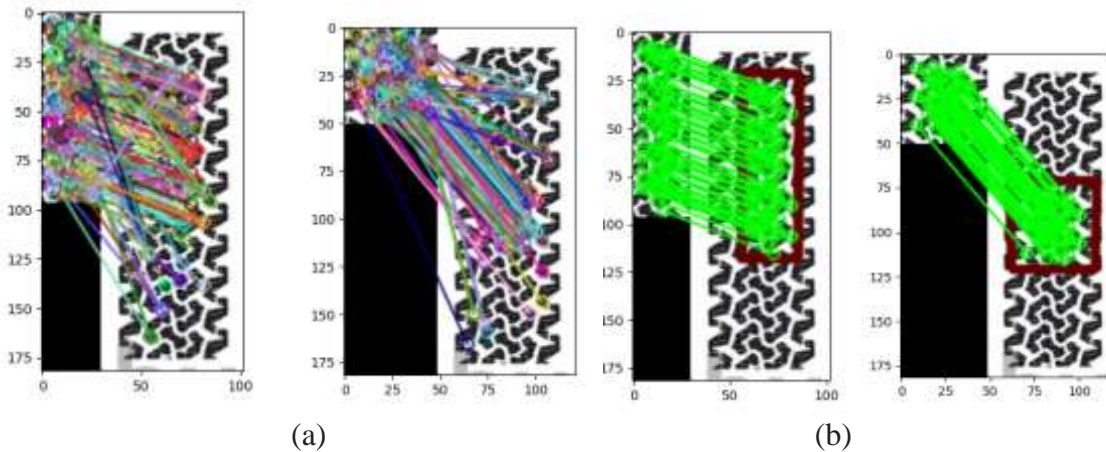


**Figure 4.** Test scenario A (a) Keypoint matches produced with SIFT, (b) Keypoint matches after outlier elimination

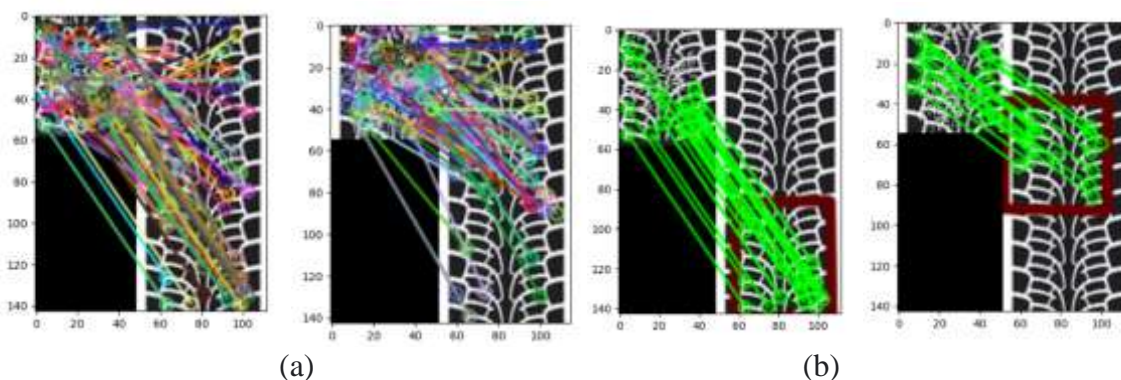


**Figure 5.** Test scenario B (a) Keypoint matches produced with SIFT, (b) Keypoint matches after outlier elimination

The tire track recognition performances of keypoint matching and template matching methods for the test scenarios A, B and C are given in Table 2. As can be seen from the table, the SIFT-RANSAC method achieved 72.38% success in matching the 105 clean track fragments with 35 clean tracks in the test scenario A, considering the first clean track with the best match. Considering

the first two (rank 2) and the first three (rank 3) clean tracks in the matching of clean track fragment, this success increased up to 84.76%. In test scenario A, 93.33% success rate was achieved with the template matching method in matching 105 clean track fragments with 35 clean tracks.

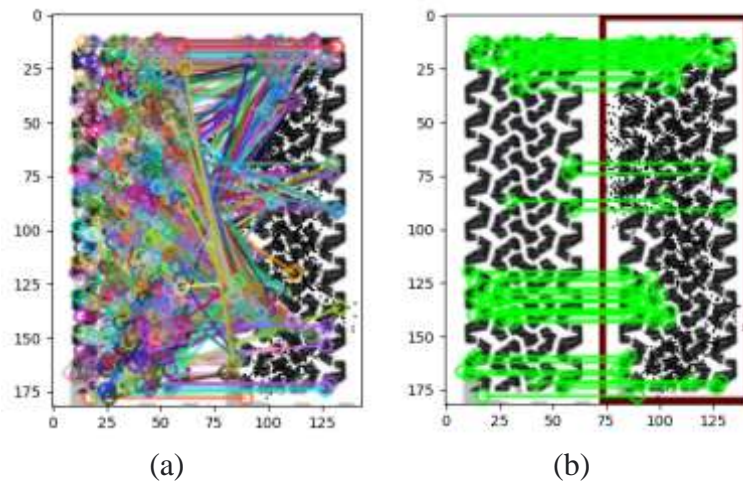


**Figure 6.** Test scenario C (a) Keypoint matches produced with SIFT ,(b) Keypoint matches after outlier elimination

In test scenario B, 31.42% success rate was obtained with the keypoints in matching 105 dirty track fragments with 35 clean tracks. Considering the first two (rank 2) and first three (rank 3) clean tracks that best match the dirty fragments, this success was only 39.04%. It can be seen that the keypoint based method is not determinative for the fragments taken from the dirty tracks, produced by randomly adding data to or subtracting data from clean tire tracks. Here, the performance can be increased by performing the noise removal process. In the same test scenario, 91.42% success rate was achieved with the template matching method.

In the final test scenario C, 35 dirty tracks were matched with 35 clean tracks. According to the results obtained, while the recognition performance with keypoints was 100%, 71.42% success was obtained with template matching.

**Table 2.** Recognition performances for test scenarios A, B and C

Test Scenario	SIFT-RANSAC	Template Matching
A	%72.38	<b>%93.33</b>
B	%31.42	<b>%91.42</b>
C	<b>%100</b>	%71.42

**Table 3.** Comparison with previous methods

Method	# of images	Accuracy
Huang ve Wang [2]	15 tire track image	%60
Bulan et al, [3]	280 tire pattern image	%97.86
Liu et al, [7]	5000 tire pattern image	%79.6
Wang et al, [9]	5000 tire pattern image	%95.9
		%93.33
Proposed method	280 tire track image	%91.42
		%100

The comparison of the study with the studies in the literature is given in Table 3. As can be seen from the table, studies in the literature generally try to recognize/classify tire images. In a study

conducted for the recognition of tire tracks, 60% success was achieved on a small number of track images. In the study, tests were carried out on different scenarios and a larger dataset was created and better classification performance was achieved.

#### 4. Conclusions

In this study, keypoint matches produced by the SIFT algorithm and template matching methods were used to classify tire tracks. The SIFT method is not affected by transformations such as translation, rotation and scaling, while high success rates have been achieved. The proposed method provides a fast and highly accurate solution for the detection and classification of tire tracks. In addition, it is seen in the study that template matching can be used for tire track recognition and classification in cases where it is necessary to work on small fragments.

In future studies, it is aimed to identify/classify tire track fragments taken from tires and real crime scenes. Applying various preprocessing techniques on tracks can improve recognition performance.

#### Authors' Contributions

VN conceived the original idea. AGY supervised the project. EI developed the application and carried out the experiments. AGY and VN discussed the results. AGY wrote the manuscript in consultation with VN. Both authors read and approved the final manuscript.

#### Competing Interests

The authors declare that they have no competing interests.

#### References

- [1]. Colbry D., Cherba D., Luchini J., "Pattern Recognition for Classification and Matching of Car Tires", *Tire Science and Technology*, 2005, 33:2-17. <http://dx.doi.org/10.2346/1.2186784>
- [2]. Huang D. Y., Hu W. C., Wang Y. W., Chen C. I., Cheng C. H., "Recognition of Tire Tread Patterns Based on Gabor Wavelets and Support Vector Machine", In: *Collective Intelligence. Technologies and Applications (ICCCI), Lecture Notes in Computer Science*, vol 6423, Springer, Berlin, Heidelberg (2010). [https://doi.org/10.1007/978-3-642-16696-9\\_11](https://doi.org/10.1007/978-3-642-16696-9_11)
- [3]. Bulan, O, Bernal, E A, Loce, R P, Wu, Wencheng, "Tire Classification from Still Images and Video", 15th International IEEE Conference on Intelligent Transportation Systems (ITSC2012), Anchorage Alaska, United States, pp 485-490, (2012).
- [4]. Wang S., Liu Y., Li D., Yan H., Bai B., "An Improved SIFT Feature Extraction Method for Tyre Tread Patterns Retrieval", 2014 Seventh International Symposium on Computer Intelligence and Design, pp. 539-543, (2014). <https://doi.org/10.1109/ISCID.2014.276>
- [5]. Liu Y., Yan H., Lim KP., "Study on rotation-invariant texture feature extraction for tire pattern retrieval", *Multidimensional Systems and Signal Processing*, 2017, 28:757-770. <https://doi.org/10.1007/s11045-015-0373-0>
- [6]. Ge Y., Liu Y., Wang F., Zhu T., Wang D., "Texture Feature Extraction Based on Histogram of Oriented Gradient Domain Texture Tendency for Tyre Pattern Retrieval", 2017 Eighth International Conference on Intelligent Control and Information Processing (ICICIP), pp.1-7, (2017). <https://doi.org/10.1109/ICICIP.2017.8113908>
- [7]. Liu Y., Zhang S., Wang F., Ling N., "Tread Pattern Image Classification using Convolutional Neural Network Based on Transfer Learning", 2018 IEEE International Workshop on Signal Processing Systems (SiPS), pp.300-305, (2018). <https://doi.org/10.1109/SiPS.2018.8598400>

- [8]. Liu Y., Zhang S., Wang F., Lim K., Liu Q., Lei Y., Gong Y., Lu J., “ Wavelet-Energy-Weighted Local Binary Pattern Analysis for Tire Tread Pattern Classification”, 2019 3rd International Conference on Imaging, Signal Processing and Communication (ICISPC), pp. 90-95, (2019). <https://doi.org/10.1109/ICISPC.2019.8935658>
- [9]. Wang F., Ding X., Liu Y., “Tyre Pattern Classification Based on Multi-scale GCN Model”, 2020 2nd Symposium on Signal Processing Systems, pp. 113-119, (2020). <https://doi.org/10.1145/3421515.3421520>
- [10]. URL: <https://www.shutterstock.com>, April 2021.
- [11]. Lowe, D. G., “Object recognition from local scale-invariant features”, Proceedings of the International Conference on Computer Vision, 2 pp.1150–1157 (1999). doi:10.1109/ICCV.1999.790410
- [12]. Lowe, D. G., “Distinctive Image Features from Scale-Invariant Keypoints”, International Journal of Computer Vision, 2004, 60(2):91–110. *CiteSeerX* 10.1.1.73.2924
- [13]. Fischler M. A., Bolles R. C., “Random Sample Consensus: A Paradigm for Model Fitting with Applications to Image Analysis and Automated Cartography”, Communications of the ACM, 1981, 24(6):381-395. <https://doi.org/10.1145/358669.358692>
- [14]. URL: [https://en.wikipedia.org/wiki/Random\\_sample\\_consensus](https://en.wikipedia.org/wiki/Random_sample_consensus), September 2021.
- [15]. Brunelli R., “Template Matching Techniques in Computer Vision: Theory and Practice”, Wiley, ISBN 978-0-470-51706-2, (2009).